ChemPubSoc Europe

DOI: 10.1002/chem.201704941

CHEMISTRY A European Journal Full Paper

Polymer Chemistry

High Surface Area, Thermally Stable, Hydrophobic, Microporous, Rigid Gels Generated at Ambient from $MeSi(OEt)_3$/$(EtO)_3SiCH_2CH_2Si(OEt)_3$ Mixtures by F^--Catalyzed Hydrolysis

Joseph C. Furgal,*[a, e] Honami Yamane,[b] Timothy R. Odykirk,[c] Eongyu Yi,[c] Yoshiki Chujo,[b] and Richard M. Laine*[c, d]

Abstract: High surface area materials are of considerable interest for gas storage/capture, molecular sieving, catalyst supports, as well as for slow-release drug-delivery systems. We report here a very simple and fast route to very high surface area, mechanically robust, hydrophobic polymer gels prepared by fluoride-catalyzed hydrolysis of mixtures of $MeSi(OEt)_3$ and bis-triethoxysilylethane (BTSE) at room temperature. These materials offer specific surface areas up to 1300 $m^2 g^{-1}$, peak pore sizes of 0.8 nm and thermal stabilities above 200 °C. The gelation times and surface areas can be controlled by adjusting the solvent volume (dichloromethane), percent fluoride (as nBu_4NF or TBAF) and the BTSE contents. Polymers with other corners and linkers were also explored. These materials will further expand the materials databank for use in vacuum insulation panels and as thermally stable release and capture media.

There is exceptional interest in developing polymeric materials with high surface areas (>750 $m^2 g^{-1}$) and microporosity (pore sizes <2 nm) driven by their potential utility in diverse applications including gas storage and/or sieving, as catalyst supports, molecular separations, insulation, low-k dielectrics, nano-reactors and release agents.[1–8] Recent active areas include the development of coordination polymers such as metal organic frameworks (MOFs) due to their minimum defect content arising from reversible chemistries and also very high surface areas (>4000 $m^2 g^{-1}$).[1,6,8]

Coincidentally, purely covalent systems, covalent organic frameworks (COFs)[9–12] have also received considerable recent attention partly because bond formation is irreversible and partly because covalent bonding makes them inherently more stable than MOFs, which rely on metal ion coordination. Two synthetic strategies used in developing COFs are via templating with porogens and the co-reaction of rigid non-planar moieties resulting in 3D structures. Many high surface area organic materials such as hyper-cross-linked styrene–divinylbenzene copolymers are made by the porogen method with surface areas approaching 2000 $m^2 g^{-1}$. Silsesquioxane based materials fit into the second synthetic methodology, whereby porosity introduction employs the monomer geometry coupled with controlled polymerization.[13–21]

Most high surface area materials containing silicon are made via sol–gel processing of tri- and tetraalkoxysilanes.[22–25] Sol–gel processing employs acid- or base-catalyzed hydrolysis and condensation to form highly cross-linked xero- or aerogels depending on the drying method. Surface areas >1000 $m^2 g^{-1}$ are easily accessible by these methods, however the long reaction times and/or critical drying conditions necessary to make these materials by sol–gel processing have prompted exploration of simple alternatives.

In a recent paper,[26] we reported that $B(C_6F_5)_3$-catalyzed Piers–Rubinsztajn oxysilylation of the cubic symmetry Q-cage $[(HMe_2SiOSiO_{1.5})_8]$ with ethoxysilanes in hexane very rapidly (minutes) forms irreversible microporous 3D networks with surface areas >700 $m^2 g^{-1}$ and peak pore sizes of ≈ 0.6 nm. One limitation to this method is its sensitivity to water. As an alternative, we sought to develop a method that offers equal or higher surface areas and is insensitive to water/moisture.

To this end, and based on our recent efforts to explore the synthesis and rearrangement of SQs by F^- catalysis.[27–29] We report here a facile method of in situ formation of high surface area microporous $MeSiOEt)_3$/bistriethoxy-silylethane (BTSE)

[a] Assist. Prof. J. C. Furgal
Department of Chemistry, University of Michigan
Ann Arbor, MI 48109 (USA)

[b] H. Yamane, Prof. Y. Chujo
Department Polymer Chemistry, Kyoto University
Kyoto, Kyoto 606-8501 (Japan)

[c] T. R. Odykirk, Dr. E. Yi, Prof. R. M. Laine
Department of Materials Science and Engineering
University of Michigan, Ann Arbor, MI 48109 (USA)
E-mail: talsdad@umich.edu

[d] Prof. R. M. Laine
Department of Macromolecular Science & Engineering
University of Michigan, Ann Arbor, MI 48109 (USA)

[e] Assist. Prof. J. C. Furgal
Department of Chemistry & Center for Photochemical Sciences
Bowling Green State University
Bowling Green, OH 43403 (USA)
E-mail: furgalj@bgsu.edu

Supporting information and the ORCID identification number(s) for the author(s) of this article can be found under https://doi.org/10.1002/chem.201704941.

based gels by F^- (as nBu_4NF)-catalyzed hydrolysis and copolymerization (yields >90%, <24 h at ambient). This work follows on complementary studies on the conversion of the same components using traditional sol–gel methods to generate extremely hard, thin films of use for nano-imprint lithography.[30]

Results and Discussion

In the following, we begin with the most basic synthesis of high surface area $[methylSiO_{1.5}]_n$/$[bis\text{-}ethylSiO_{1.5}]_m$ polymer gels by F^- catalysis (Scheme 1). These materials are very simple to make, $MeSi(OEt)_3$ and bis-triethoxysilylethane (BTSE) are added to a flask containing CH_2Cl_2, followed by small amounts of water and finally 1 M TBAF solution as catalyst (Table 1). The solution is left to stir, producing white precipitates (network polymer) within one hour. After 24 h, the precipitates are filtered off, rinsed and dried under vacuum at 50 °C. These precipitates were then characterized by FTIR (see Supporting Information), TGA, scanning electron microscopy (SEM) and XRD) and their specific surface areas (SSAs) analyzed by Brunauer–Emmett–Teller (BET).

Initial experiments adjusted $MeSi(OEt)_3$/BTSE ratios to determine how cross-link densities affected SSAs. As seen in Table 1 for gels **1–4**, small changes ±2 mmol in BTSE only minimally influence SSAs, providing materials with SSAs ≈1000 m^2g^{-1}. Halving the reaction scale (gels **6–10**) and increasing the F^- concentration from 0.08 to 0.12 equivalents increases SSAs slightly to 1300 m^2g^{-1} (Table 1, gel 7), higher than most zeolites.[31–37] The effect of water on the reaction was explored, however no clear trend was observed. FTIR analyses (Figure S1) of these materials showed only small νC–H (3000 cm^{-1}) suggesting elimination of ethoxy groups, resulting from complete formation of $RSiO_{1.5}$ species likely consisting of complete and partly ring opened SQ cages.[22,23]

Thermal analysis using TGA/DTA was somewhat complicated by the high porosity and friability of these materials, with the air flow in TGA analysis often blowing powders out of the ceramic pans. Still a further issue is that some solvent or residual ethoxy groups might remain trapped in pores even despite drying such that initial mass losses though small may arise from very slow release of this residual solvent or water as it works its way through torturous paths.

Nonetheless, several successful runs were obtained allowing interpretation of extent of polymerization and thermal stability. Figure 1 shows an exemplary TGA of gel **7** revealing a thermal stability, defined as a 5 wt% mass loss temperature of 395 °C.

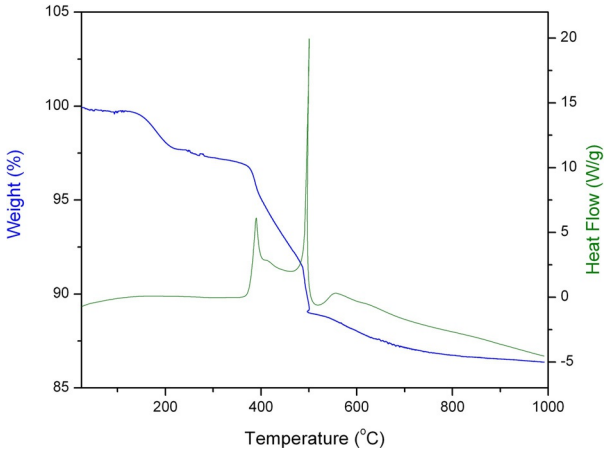

Figure 1. TGA/DTA of gel **7**. Theoretical ceramic yield (CY) of 90% and actual CY of 87%.

The actual and theoretical ceramic yields, 87 versus 90% respectively may be attributable to residual solvent, water or incomplete removal of the ethoxy groups as noted just above.

These results can be anticipated based on polymer formation coincident with precipitation. Precipitation will result in greatly reduced reaction rates. Certainly, diffusion rates must be curtailed by the very fine pore structures. This is the most likely scenario for retaining (trapping) small amounts of ethoxy groups. Even so, this is relatively small if we assume the mass loss just above 200 °C is from ethoxy groups, it amounts to ≈2 wt%. A thermal anneal at 200 °C would alleviate this discrepancy forcefully removing the remaining ethoxy groups.

The Figure 2 XRD shown for gel **7** shows little to no periodicity. The only clear peak at ≈23° 2θ is typical of an amorphous hump but it also corresponds to the separation between cage faces (≈0.4 nm).[38] These results were anticipated

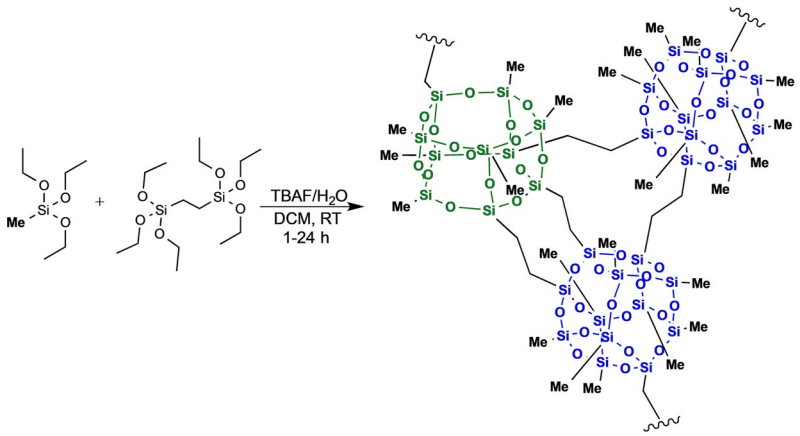

Scheme 1. Reaction of $MeSi(OEt)_3$ w/BTSE using TBAF as catalyst in CH_2Cl_2 as solvent.

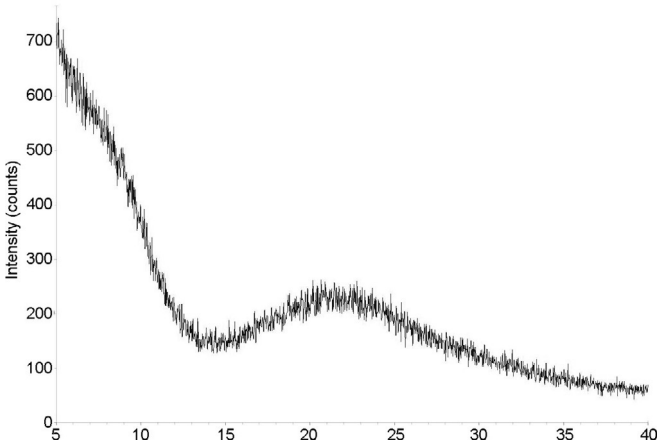

Figure 2. XRD of gel **7** showing that the material is amorphous.

and contrast with those exhibited by zeolites because the reaction is a kinetic precipitation method at room temperature, whereas zeolites are hydrothermally equilibrated to form crystalline structures.[32,33]

Scanning electron microscopy images of gel **7** (Figure 3) reveal a tendency to agglomerate, typical of fine powders. Overall the method gives materials with quite uniform particle shapes and sizes.

Micropore/mesopore analysis of gel 7 (Figure 4) shows peak pore diameters of $\approx$0.8 nm, (Figure 4a) and a cumulative pore volume of 2.3 $cm^3 g^{-1}$ (Micro- and *meso*-pore volumes, 0.42 and 1.92 $cm^3 g^{-1}$, respectively). Since the pore diameters have a reasonably narrow distribution, it would be expected that the formed structures are uniform. For these materials, retention of high SSA does not necessitate supercritical processing, which means no extensive pore collapse is observed on

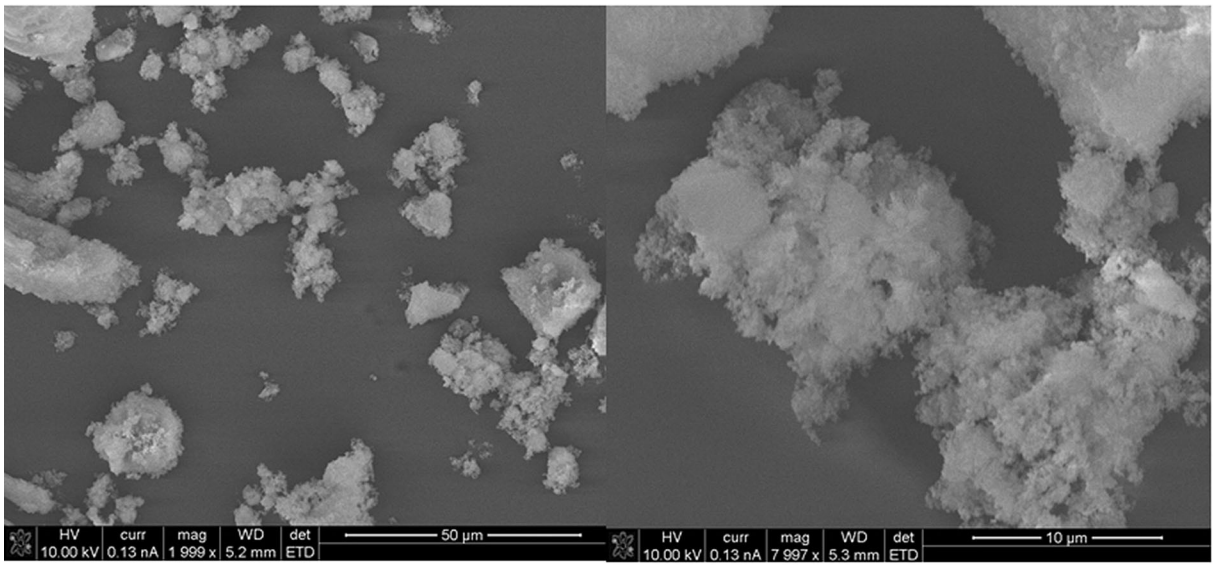

Figure 3. SEM images of gel **7** at 2000× and 8000× magnification.

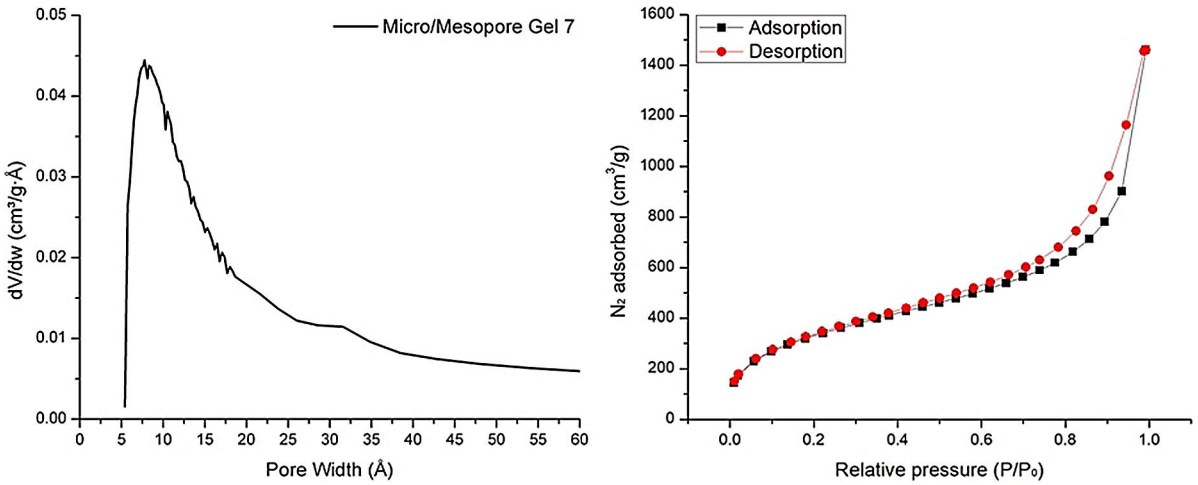

Figure 4. a) Micro/mesoporosimetry BJH/Horvath–Kawazoe differential pore volume plot for gel **7** at $0 \leq p/p_0 \leq 0.1$ showing peak pore size of $\approx$1.0 nm, b) BET mesopore analysis of gel **7** showing N_2 adsorption up to 1500 $cm^3 g^{-1}$ with a type II shape and H3 hysteresis loop with slit-like pores.[40].

drying. Efforts to measure pore sizes and pore volumes show that the materials are in general very similar as seen in Table 1. Thus, extensive measurements of all samples were considered unnecessary.

Porous materials with pore sizes in both mesoporous and microporous ranges often exhibit hysteresis during gas adsorption measurements. Interconnected pore systems containing pore blockages often cause a lag in desorption of gas from the material at $p/p_0 = 0.45$ (N_2 at 77 K), see Figure 4b, in agreement with literature.[39] Due to this, porosity measurements are taken from the adsorption instead of desorption stage, which is less affected by hysteresis. However, note in gel **7** that only slight hysteresis is observed in the type II isotherm between the adsorption and desorption curves from 0.6 to 1.0 p/p_0, and the curves nearly overlap.[40] This would suggest that there are few pore blockages in the materials. The shape of this hysteresis (Type H3) suggests that we have slit shaped pores.

Compression, density and solvent uptake studies were also conducted on these materials. The bulk density was of the order of aerogels, 0.06 g cm^{-3} (gel **7**) as might be expected based on their high porosity.[22] Attempts to compress recovered dried powders into pellets using a die press were thwarted due to their inherent flowability, with the material squeezing past the die, or retaining its texture after more than 13800 kPa of pressure was applied. Further attempts using a relatively crude test resulted in some densification of the sample (Figure 5), climbing to 0.15 g mL^{-1} at ≈9 kPa of pressure.

Table 1. Solvent uptake studies using gel **7**.

Solvent	Mass solvent	Mass gel	≈Uptake
hexanes	135 mg	22 mg	560%
tetrahydrofuran	95 mg	17 mg	600%
water	N/A	N/A	N/A

Simple solvent uptake studies were also performed, comparing hexanes, THF and water. The methyl groups and ethyl bridges in these materials give them strongly hydrophobic properties; therefore only organic solvents were "soaked up", with hexanes studies giving 560% mass:mass solvent uptake and THF giving 600% solvent uptake per mass of gel (Table 1). The gel ran up the sides of the vials in tests with water, showing no interaction or water uptake. This suggests that these materials may be useful as molecular sponges for oil/water separation.[25]

To add utility to these materials and study the influence of other R-functional groups on the SSA of the system, further reaction analyses were conducted by varying the above reaction conditions and also studying the incorporation of vinylSi(OEt)$_3$ and PhSi(OEt)$_3$ (Scheme 2). Table 2 shows the results of these studies and FTIR characterization given in Figures S2–S9.

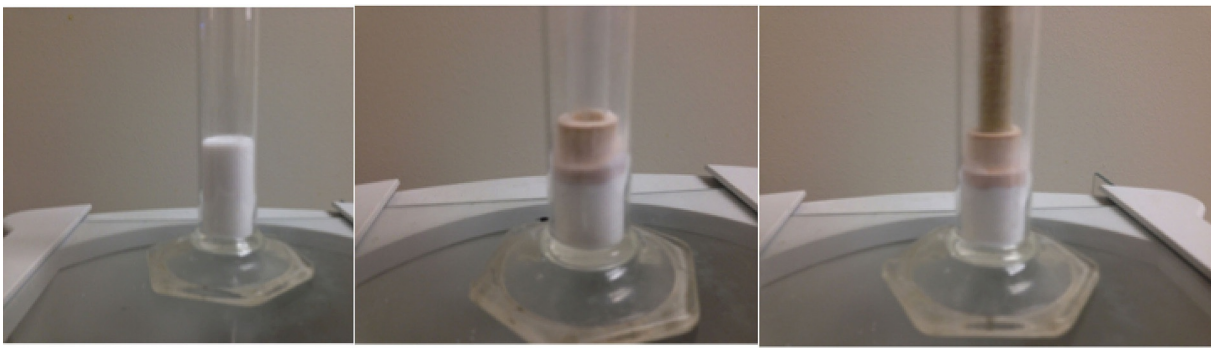

Figure 5. Efforts to compress gel **7**. a) uncompressed density 0.06 g mL^{-1}, 719 mg powder fills 10 mL; b) Density under a 5 g wt. = 0.12 g mL^{-1} (719 mg powder in 5.8 mL); c) Density under 300 g wt. (9 kPa), 0.15 g mL^{-1} 719 mg powder in 4.9 mL.

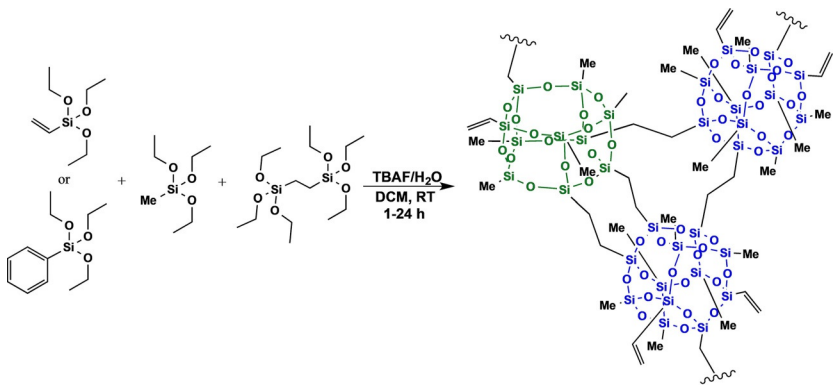

Scheme 2. TBAF-catalyzed reaction: vinylSi(OEt)$_3$ or PhSi(OEt)$_3$ and MeSi(OEt)$_3$ w/BTSE.

Table 2. F^--catalyzed co-condensation of $MeSi(OEt)_3$/BTSE/$RSi(OEt)_3$ (R = vinyl, phenyl).

	$MeSi(OEt)_3$ [mmol]	BTSE [mmol]	TBAF [mmol]	DI water [mL]	CH_2Cl_2 [mL]	$VinylSi(OEt)_3$ [mmol]	$PhenylSi(OEt)_3$ [mmol]	SSA [$m^2 g^{-1}$]
12	25.1	8.8	6.9	3	50	–	–	745
13	25.1	8.8	6.9	3	100	–	–	651
14	25.1	8.8	6.9	3	200	–	–	660
15	25.1	8.8	6.9	3	400	–	–	880
16	12.5	4.5	5.2	1.5	400	–	–	578
17	12.5	3.5	5.2	1.5	400	–	–	835
18	12.5	3	5.2	1.5	400	–	–	605
19	12.5	2	5.2	1.5	400	–	–	805
20	15.1	8.8	6.9	3	400	13.1	–	691
21	20.1	8.8	6.9	3	400	6.5	–	880
22	22.6	8.8	6.9	3	400	3.3	–	947
23	23.8	8.8	6.9	3	400	1.6	–	742
24	24.8	8.8	6.9	3	400	0.33	–	834
25	7.53	4.4	1.5	1.5	400	4.7	–	910
26	0	8.8	6.9	3	400	–	20.7	345
27	12.5	8.8	6.9	3	400	–	10.4	688
28	22.6	8.8	6.9	3	400	–	2.1	785

At present, it appears that introducing small amounts of another R group do not lead to sacrifices in SSAs but these studies are very preliminary and simply provide the basis for further studies especially where R is a functional group used for example to introduce a catalyst, a drug, a point to capture trace metals or pollutants. Thus, the above initial studies lay the groundwork for practical efforts.

Conclusion

Fluoride-catalyzed hydrolysis–condensation methods offer a unique route to high SSA materials based on methylsilsesquioxane. In general, the resulting gels are stable to $>250\,^{\circ}C$ and offer very low densities of 0.1–0.2 $g\,mL^{-1}$, similar to aerogels. Gel materials offer SSA's of up to 1300 $m^2 g^{-1}$ some of the highest known systems based on SQs.[15–24] Gel materials also offer solvent uptake up to 600% by mass. Vinyl groups can be incorporated into the systems offering post polymerization functionalization points and further crosslink density, extending the useful possibilities for these materials. These materials offer excellent possibilities for use in vacuum insulation panels and as thermally stable release and capture media.

Experimental Section

Materials

Methyltriethoxysilane [$MeSi(OEt)_3$], vinyltriethoxysilane [$vinyl-Si(OEt)_3$], phenyltriethoxy-silane [$PhSi(OEt)_3$] and bistrithoxysilylethane [$(EtO)_3SiCH_2CH_2Si(OEEt)_3$, BTSE] were obtained from Gelest, Inc. Phenyl T_{10}/T_{12} silsesquioxane (dodecaphenyl silsesquioxane or DDPS) was made in house. Tetrahydrofuran (THF), and tetrabutylammonium fluoride (TBAF, 1.0 M in THF) were obtained from Sigma–Aldrich. All chemicals were used as received. All reactions were conducted at room temperature in the presence of air.

Table 3. F^--catalyzed co-condensation of $MeSi(OEt)_3$/BTSE to form high surface area materials.

Entry	$MeSi(OEt)_3$ [mmol]	BTSE [mmol]	TBAF [mmol]	H_2O [mL]	CH_2Cl_2 [mL]	Surface area [$m^2 g^{-1}$]	Peak pore size	Cumulative pore volume
1	25.1	8.11	2.0	3.0	800	875	–	–
2	25.1	8.78	2.0	3.0	800	1040	–	–
3	25.1	7.43	2.0	3.0	800	1034	–	–
4	25.1	9.46	2.0	3.0	800	1049	–	–
5	25.1	8.78	2.0	3.2	800	1188	–	–
6	12.5	5.07	1.0	1.7	400	1144	0.8 nm	1.44 $cm^3 g^{-1}$ [0.37 micro/1.07 *meso*]
7	**12.5**	**4.39**	**1.5**	**1.5**	**400**	**1307**	0.8 nm	2.34 $cm^3 g^{-1}$ [0.42 micro/1.92 *meso*]
8	12.5	4.39	0.5	1.5	400	1194	0.8 nm	1.97 $cm^3 g^{-1}$ [0.39 micro/1.58 *meso*]
9	12.5	4.39	1.0	2.0	400	1242	–	–
10	12.5	4.39	1.0	1.0	400	1145	–	–
11	25.1	0	2.0	2.5	800	4	–	–

Typical condensation reactions

In a 1 L round bottom flask equipped with magnetic stirring were mixed 800 mL of reagent grade CH_2Cl_2, and 12 to 25 mmol of Me-$Si(OEt)_3$ and 8–4 mmol of BTSE. To this mixture was added 1–3 mL of H_2O and 0.5–2 mmol of TBAF in CH_2Cl_2 and the reaction stirred for 24 h at ambient under air. Table 3 lists sets of experiments conducted a minimum of two times.

Analytical methods

Fourier- transform infrared spectroscopy (FTIR)

Diffuse reflectance Fourier transform (DRIFT) spectra were obtained using a Nicolet 6700 Series FTIR spectrometer (Thermo Fisher Scientific, Inc., Madison, WI). Optical grade KBr (International Crystal Laboratories, Garfield, NJ) was ground with 1.0 wt% of the sample to be analyzed. The ground powder was packed into a sample holder and leveled off with a glass plate to give a smooth surface. The FTIR sample chamber was purged continuously with N2 prior to data acquisition. 64 scans were averaged for each spectrum in the range 4000-400 cm^{-1} with a precision of $\approx 4\,cm\,cm^{-1}$.

Specific surface area (SSA) and porosity analyses

Were carried out using an ASAP 2020 sorption analyzer (Micromeritics Inc., Norcross, GA). Samples (200 mg) were degassed at 150 °C/8 h. Each analysis was run at Å196 °C (77 K) with N2. The SSAs were determined by the BET multipoint method using ten data points at relative pressures (p/p_0) of 0.050.30. The micropore size distribution was determined by the Horvath-Kawazoe method. Data points were collected with low pressure incremental dose mode at $0 < p/p_0 \leq 0.1$. Mesopore size distributions were calculated using the BJH method from data points collected at $0 < p/p_0 \leq 1.0$.

Thermal gravimetric analysis (TGA/DTA)

Thermal stabilities of materials under synthetic air were measured on a Q600 simultaneous TGA-DSC Instrument (TA Instruments, Inc., New Castle, DE). Before analysis, samples were ground into a powder and 15–25 mg were placed into alumina pans and then ramped from 25 to 1000 °C (10 °C min^{-1}). The air-flow was 60 mL min^{-1}.

X-ray diffraction

XRD patterns were collected on a Rigaku Rotating Anode Goniometer (Rigaku Denki., LTD., Tokyo, Japan). The Jade Program 2010 (Version 1.1.5 Materials Data, Inc., Livermore CA) was used to determine the presence of crystallographic phases. XRD scans were made from 5 to 40° 2θ, using a scan rate of 0.5° min^{-1} in 0.01° increments (2° min^{-1} for those in Supporting Information) and $Cu_{K\alpha}$ radiation (1.541 Å) operating at 40 kV and 100 mA.

Scanning electron microscopy

Micrographs were taken using a FEI NOVA Nanolab system (FEI company, Hillsboro, OR) at mode 2. Samples were sputter coated with gold/palladium using a Technics Hummer IV DC sputtering system (Anatech, Ltd., Alexandria, VA) to prevent charging.

Solvent impregnation studies

Gels (500–600 mg) were ground into powders and dried in air for 30 min at 100 °C. Powders were cooled to ambient and weighed. Powders were then placed in a clean beaker and covered with 20 mL of reagent grade solvent for 30 min. The mixture was then gravity filtered and the powders patted dry with a Kimwipe and air-dried for 10 min before weighing. Solvent mass retention was calculated from the difference between wet and dry mass using the following formula: mass gain $= mass_{wet} - mass_{dry}/mass_{dry} \times 100\,\%$.

Acknowledgements

We would like to thank Intel for support of the work reported here through Semiconductor Research Corporation (MSR) Task 2170.001.

Conflict of interest

The authors declare no conflict of interest.

Keywords: gels · high surface area · hydrolysis · materials chemistry · polymers

[1] O. M. Yaghi, H. Li, C. Davis, D. Richardson, T. L. Groy, *Acc. Chem. Res.* **1998**, *31*, 474 – 484.
[2] S. Inagaki, S. Guan, Y. Fukushima, T. Ohsuna, O. Terasaki, *J. Am. Chem. Soc.* **1999**, *121*, 9611 – 9614.
[3] J. Y. Ying, C. P. Mehnert, M. S. Wong, *Angew. Chem. Int. Ed.* **1999**, *38*, 56 – 77; *Angew. Chem.* **1999**, *111*, 58 – 82.
[4] A. Stein, B. J. Melde, R. C. Schroden, *Adv. Mater.* **2000**, *12*, 1403 – 1419.
[5] F. Schüth, *Chem. Mater.* **2001**, *13*, 3184 – 3195.
[6] M. Eddaoudi, D. B. Moler, H. Li, B. Chen, T. M. Reineke, M. O'Keeffe, O. M. Yaghi, *Acc. Chem. Res.* **2001**, *34*, 319 – 330.
[7] G. J. D. Soler-Illia, C. Sanchez, B. Lebeau, J. Patarin, *Chem. Rev.* **2002**, *102*, 4093 – 4138.
[8] H.-C. Zhou, J. R. Long, O. M. Yaghi, *Chem. Rev.* **2012**, *112*, 673 – 674.
[9] M. Mastalerz, *Angew. Chem. Int. Ed.* **2008**, *47*, 445 – 447; *Angew. Chem.* **2008**, *120*, 453 – 455.
[10] H.-B. Yang, K. Ghosh, A. M. Arif, P. J. Stang, *J. Org. Chem.* **2006**, *71*, 9464 – 9469.
[11] H. Menzel, M. D. Mowery, M. Cai, C. E. Evans, *Macromolecules* **1999**, *32*, 4343 – 4350.
[12] S.-Y. Ding, W. Wang, *Chem. Soc. Rev.* **2013**, *42*, 548 – 556.
[13] C. Zhang, F. Babonneau, C. Bonhomme, R. M. Laine, C. L. Soles, H. A. Hristov, A. F. Yee, *J. Am. Chem. Soc.* **1998**, *120*, 8380 – 8391.
[14] Y. Kim, K. Koh, M. F. Roll, R. M. Laine, A. J. Matzger, *Macromolecules* **2010**, *43*, 6995 – 7000.
[15] M. F. Roll, J. W. Kampf, Y. Kim, E. Yi, R. M. Laine, *J. Am. Chem. Soc.* **2010**, *132*, 10171 – 10183.
[16] D. Wang, L. Xue, L. Li, B. Deng, S. Feng, H. Liu, X. Zhao, *Macromol. Rapid Commun.* **2013**, *34*, 861 – 866.
[17] D. Wang, W. Yang, L. Li, X. Zhao, S. Feng, H. Liu, *J. Mater. Chem. A* **2013**, *1*, 13549 – 13558.
[18] F. Alves, I. Nischang, *Chem. Eur. J.* **2013**, *19*, 17310 – 17313.
[19] Y. Wu, D. Wang, L. Li, W. Yang, S. Feng, H. Liu, *J. Mater. Chem. A* **2014**, *2*, 2160 – 2167.
[20] C. J. Brinker, G. W. Scherer, *Sol-Gel Science: The Physics and Chemistry of Sol-Gel Processing*, Academic press, **1990**.
[21] Z. Zhang, P. Zhang, Y. Wang, W. Zhang, *Polym. Chem.* **2016**, *7*, 3950 – 3976.
[22] Y. Li, X.-H. Dong, Y. Zou, Z. Wang, K. Yue, M. Huang, H. Liu, X. Feng, Z. Lin, W. Zhang, et al., *Polymer* **2017**, *125*, 303 – 329.
[23] D. A. Loy, K. J. Shea, *Chem. Rev.* **1995**, *95*, 1431 – 1442.
[24] H. W. Oviatt, Jr., K. J. Shea, J. H. Small, *Chem. Mater.* **1993**, *5*, 943 – 950.
[25] C. M. Burkett, L. A. Underwood, R. S. Volzer, J. A. Baughman, P. A. Edmiston, *Chem. Mater.* **2008**, *20*, 1312 – 1321.
[26] P. H. Doan, E. Yi, J. C. Furgal, M. Schwartz, S. Clark, T. Goodson III, R. M. Laine, *J. Ceram. Soc. Jpn.* **2015**, *123*, 756 – 763.

[27] M. Z. Asuncion, R. M. Laine, *J. Am. Chem. Soc.* **2010**, *132*, 3723 – 3736.
[28] J. C. Furgal, J. H. Jung, S. Clark, T. Goodson III, R. M. Laine, *Macromolecules* **2013**, *46*, 7591 – 7604.
[29] J. C. Furgal, T. Goodson III, R. M. Laine, *Dalton Trans.* **2016**, *45*, 1025.
[30] H. W. Ro, V. Popova, L. Chen, A. M. Forster, Y. Ding, K. J. Alvine, D. J. Krug, R. M. Laine, C. L. Soles, *Adv. Mater.* **2011**, *23*, 414 – 420.
[31] E. M. Flanigen, J. M. Bennett, R. W. Grose, J. P. Cohen, R. L. Patton, R. M. Kirchner, J. V. Smith, *Nature* **1978**, *271*, 512 – 516.
[32] R. M. Barrer, *Hydrothermal Chemistry of Zeolites*, Academic Press, London, **1992**.
[33] M. L. Occelli, H. Kessler, *Synthesis of Porous Materials*, Marcel Dekker, New York, **1997**.
[34] B. Naik, N. N. Ghosh, *Recent Pat. Nanotechnol.* **2009**, *3*, 213 – 224.
[35] T. Yanagisawa, T. Shimizu, K. Kuroda, C. Kato, *Bull. Chem. Soc. Jpn.* **1990**, *63*, 988 – 992.
[36] C. T. Kresge, M. E. Leonowicz, W. J. Roth, J. C. Vartuli, J. S. Beck, *Nature* **1992**, *359*, 710 – 712.
[37] J. S. Beck, J. C. Vartuli, W. J. Roth, M. E. Leonowicz, C. T. Kresge, K. D. Schmitt, C. T-W. Chu, D. H. Olson, E. W. Sheppard, S. B. McCullen, J. B. Higgins, J. L. Schlenker, *J. Am. Chem. Soc.* **1992**, *114*, 10834 – 10843.
[38] D. B. Cordes, P. D. Lickiss, R. Franck, *Chem. Rev.* **2010**, *110*, 2081 – 2173.
[39] M. Thommes, B. Smarsly, M. Groenewolt, P. I. Ravikovitch, A. V. Neimark, *Langmuir* **2006**, *22*, 756 – 764.
[40] K. S. W. Sing, D. H. Everett, R. A. W. Haul, L. Moscou, R. A. Pierotti, J. Rouquerol, T. Siemieniewska, *Pure Appl. Chem.* **1985**, *57*, 603 – 619.

Manuscript received: October 18, 2017
Accepted manuscript online: October 20, 2017
Version of record online: November 29, 2017